Proceedings of the ASME 2010 3rd Joint US-European Fluids Engineering Summer Meeting and 8th International Conference on Nanochannels, Microchannels, and Minichannels
FEDSM-ICNMM2010
August 1-5, 2010, Montreal, Canada

FEDSM-ICNMM2010-30418

PERFORMANCE AND FLOW CONDITIONS OF CONTRA-ROTATING SMALL-SIZED AXIAL FAN

Toru SHIGEMITSU
Institute of Technology and Science
The University of Tokushima
Tokushima, Japan
t-shige@me.tokushima-u.ac.jp

Junichiro FUKUTOMI
Institute of Technology and Science
The University of Tokushima
Tokushima, Japan
fukutomi@me.tokushima-u.ac.jp

Yuki OKABE
Graduate School of Advanced Technology and Science
The University of Tokushima
Tokushima, Japan

Kazuhiro IUCHI
Graduate School of Advanced Technology and Science
The University of Tokushima
Tokushima, Japan

ABSTRACT

Small-sized axial fans are used as air cooler for electric equipments. But there is a strong demand for higher power of fans according to the increase of quantity of heat from electric devices. Therefore, higher rotational speed design is conducted although, it causes the deterioration of efficiency and the increase of noise. Then the adoption of contra-rotating rotors for the small-sized axial fan is proposed for the improvement of performance. In the present paper, the performance curves of the contra-rotating small-sized axial fan with 100mm diameter are shown and the velocity distributions for a designed flow rate at the inlet and the outlet of each front and rear rotor are clarified with experimental results. Furthermore, the flow conditions between front and rear rotors of the contra-rotating small-sized axial fan are investigated by numerical analysis results and higher performance design of the contra-rotating small-sized axial fan is discussed.

INTRODUCTION

There is a strong demand for higher efficiency of data centers and electric devices to take one role for solving energy problem and global warming because the consumption of the electrical power has been increasing significantly according to the spread of cloud computing, the establishment of ubiquitous networking society and the increase of quantity of heat from electric devices[(1)]. Electrical power used for the cooling of the IT devices for data centers is huge the same as that used for the IT devices itself in data centers. Small-sized axial fans are used as air coolers for electric equipments i.e. laptop, desk top computers and servers. There is a strong demand for higher power of fans according to the increase of quantity of heat from electric devices. However, the increase of the power by the increase of the fan diameter is restricted because of the limitation of the space. Therefore, higher rotational speed design is conducted, although it causes the deterioration of the efficiency and the increase of noise. On the other hand, lower rotational speed design[(2)] and advantages on the performance of the contra-rotating fans and pumps are verified by experimental results[(3),(4)]. Then the adoption of contra-rotating rotors for small-sized fans is proposed for the improvement of the performance. In the case of contra-rotating rotors, the axial space becomes larger than conventional small-sized axial fans. However, it is adequate choice to apply the contra-rotating rotors for small sized-fans because the axial space can be

ensured in electrical devices as compared to that of the radial space.

In the case of contra-rotating rotors, it is necessary to design rear rotor considering the unsteady circumferential velocity distributions at the outlet of the front rotor[5]. And it is important to clarify the influence of the wake from the front rotor to the rear rotor on the performance and pressure interaction between front and rear rotors[6]. On the other hand, the conventional design method and the theory for the turbo machinery should be modified for small-sized axial fans because small-sized axial fans applied to electrical devices belong to extremely small size field in the turbo machinery[7]. Therefore, there is the strong demand to establish the design method for small-sized axial fans.

In the present paper, the performance curve of the contra-rotating small-sized axial fan with 100mm diameter is shown and the internal flow conditions at the designed flow rate are clarified by experimental results. Furthermore, the relations between the performance and flow conditions were discussed by the experimental and numerical results and the rear rotor design to improve the performance of contra-rotating small-sized axial fan is considered.

NOMENCLATURE

A	Sectional area of the rotor $=\pi D_t^2/4$ (m^2)
D_h	Hub diameter (m)
D_t	Tip diameter (m)
L	Shaft power (W)
l	Hub chord length of the rear rotor(m)
N	Rotational speed (min^{-1})
N_f	Rotational speed of the front rotor (min^{-1})
N_r	Rotational speed of the rear rotor (min^{-1})
P_d	Dynamic pressure(Pa)
P_s	Static pressure (Pa)
P_t	Total pressure (Pa)
ΔP	Fan static pressure (Pa)
ΔP_{dR}	Designed fan static pressure of conventional small-sized axial fan (Pa)
ΔP_{dRR}	Designed fan static pressure of contra-rotating small-sized axial fan (Pa)
Q	Flow rate (m^3/s)
R	Radius (m)
r_c	Radius at the casing (m)
U	Circumferential speed of the rotor $=\pi D_t N/60$ (m/s)
U_{RR}	Circumferential speed of the rotor for RRtype $=\pi D_t N_r/60$ (m/s)
V_t	Circumferential component of absolute velocity (m/s)
V_z	Axial component of absolute velocity (m/s)
Z	Axial distance (m)
ρ	Density of air (kg/m^3)
η	Static pressure efficiency$=\Delta PQ/L$

EXPERIMENTAL APPARATUS AND NUMERICAL METHOD

The rotor and the primary dimensions of a conventional axial fan(Rtype) and a contra-rotating axial fan(RRtype) are shown in Fig.1 and Table 1 respectively. The hub tip ratio D_h/D_t=45mm/98mm and the designed flow rate was Q_d=0.016m^3/s for both types and fan static pressure at the design point was ΔP_{dR}=13.7Pa for Rtype and ΔP_{dRR}=14.7Pa for RRtype with the same fan static pressure of each front and rear rotor. The rotational speed of Rtype was N=3000min^{-1}. On the other hand, the rotational speed of each front and rear rotor of RRtype was N_f=N_r=1780min^{-1} in order to make the specific speed of each rotor for RRtype became almost the same with Rtype. In this research, an aerofoil blade was used because there was a report which told an advantage of the aerofoil blade for the small-sized axial fan[8], however a circular-arc blade was generally used for small-sized axial fans. RRtype rotor used for the experiment was changed a little from the rotor for the numerical analysis in the blade thickness and so on under the condition of the same designed performance because the thickness for the numerical analysis rotor was thin and the lack of the strength for using it for the experiment was worried. Figure 2 shows the schematic diagram of the experimental apparatus for RRtype. The experimental apparatus was designed based on the Japanese Industrial Standard and the air blown in the test section passed the rotor, chamber, measurement duct and booster fan and blew out in the ambient atmosphere. The fan static pressure (ΔP) was measured by the pressure difference between static holes downstream of the rotor installed at the chamber and ambient air. Further, the rotational speed was controlled by the servo motor and the flow rates were measured by the orifice meter set at the measurement duct. The pressure curves from the cutoff flow rate to the large flow rate were investigated in the experiment with the constant rotational speed N_f=N_r=1780min^{-1} for RRtype and N=3000min^{-1} for Rtype. The internal flow measurements at the inlet and the outlet of each rotor were conducted with a one-hole cylindrical pitot tube having an outer diameter of 2.0mm. This tube was used as the substitution of a three-hole pitot tube by rotating it by ±30°. The measurements in axial direction were conducted from 5mm upstream of the leading edge of the front rotor at the

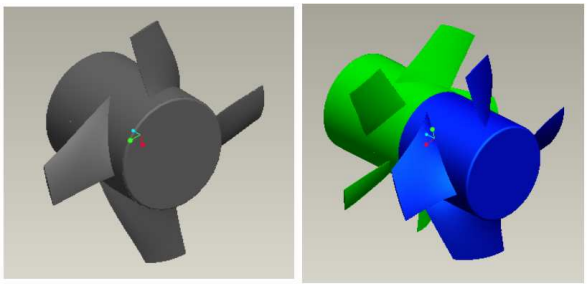

(a) Rtype (b) RRtype

Fig.1 Small-sized axial fan

hub to 4 other axial upstream positions by interval of 10mm at the inlet of the front rotor, at 5mm downstream of the trailing edge of the front rotor at the hub to 4 other axial downstream positions by interval of 5mm at the outlet of the front rotor and at 6mm downstream of the trailing edge of the rear rotor at the hub, from 40mm downstream of the trailing edge of it to 6 other axial downstream positions by interval of 10mm at the outlet of the rear rotor. Further, the measurements in radial direction were conducted from r=28.5mm to r=49.5mm by interval of 3mm at 8 radial positions. Therefore, the total of the measurements points were 144 points.

The commercial software ANSYS-Fluent was used to investigate the flow condition which couldn't be measured by the experiment. In the numerical analysis, the numerical model which was almost the same with the experimental apparatus was used and three dimensional steady numerical analysis was conducted. The numerical grids used for the numerical analysis are shown in Fig.3. The numerical domains were comprised of the inlet, rotor, chamber and outlet duct regions. The numerical grids number at each region are 218,039 for the inlet region, 1,521,481 in the case of Rtype and 3,613,381 in the case of RRtype for the rotor region, 667,135 for the chamber region and 39,875 for the outlet duct region respectively. The number of nodes along the front and the rear rotor blades at the hub were 150 nodes and 80 nodes. The number of nodes of blade-to-blade of the front and the rear rotors were 35 nodes and 30 nodes. The number of nodes from hub to tip of the front and the rear rotors were 110 nodes and 100 nodes. The tip clearance was kept 1mm as the same with the experimental apparatus in the numerical analysis and the number of nodes from the blade tip to the casing was 7 nodes. The numerical grids over 150,000 were ensured at the tip clearance. The y^+ was 15 near the hub of the rotor. At the inlet boundary, the uniform velocity was given and the constant pressure was given as the outlet boundary condition. The coupling between the front and the rear rotors was accomplished by the frozen rotor method with multiple reference frames. The standard wall function and k-ω turbulence model was used. The standard wall function was used on blades, casing wall and chamber wall. The numerical flow analysis was conducted at the 6 different flow rates from $0.6Q_d$ to $1.2Q_d$.

EXPERIMENTAL AND NUMERICAL RESULTS

Figure 4(a) shows the pressure curves of Rtype and RR type obtained by the experiment. The shaft power and the efficiency of Rtype and RRtype obtained by the numerical analysis are shown in Fig.4(b). In Fig.4(a), the pressure curves obtained by the numerical analysis are also shown to compare with the experimental results. The dimensional values were used for the performance curves to compare the performance of Rtype and RRtype clearly in Fig.4. It could be found that the fan pressure increased according to the decrease of the flow rates and the pressure curves showed the stable negative curve from the experimental results of both Rtype and RRtype. Further, numerical results represented the qualitative tendency of the experimental results. The fan static pressure of Rtype and RRtype were ΔP=7.5Pa and ΔP=10.0Pa at the designed flow rate Q_d=0.016m^3/s. The fan pressure of RRtype was higher than that of Rtype in wide flow rate range from $0.4Q_d$ to $1.1Q_d$ and an advantage of RRtype could be confirmed that high fan pressure could be obtained for RRtype. However, the fan pressure of RRtype was lower than Rtype near shut off flow rate and over flow rate $1.2Q_d<Q$. Further, the fan pressures of Rtype and RRtype at the designed flow rate were lower than designed

Table 1 Primary dimensions of R and RRtypes

		Hub	Mid	Tip
Rotor (Rtype)	Diameter[mm]	45	72	98
	Blade Number	4		
	Blade Profile	NACA4412		
	Solidity	0.908	0.361	0.208
	Stagger Angle	59.84°	60.11°	74.87°
Front Rotor (RRtype-exp.)	Blade Number	4		
	Blade Profile	NACA4409		
	Solidity	1.196	0.496	0.29
	Stagger Angle	44.67°	61.09°	68.15°
Rear Rotor (RRtype-exp.)	Blade Number	5		
	Blade Profile	NACA4412		
	Solidity	0.91	0.447	0.288
	Stagger Angle	56.73°	64.54°	69.60°
Front Rotor (RRtype-cal.)	Blade Number	4		
	Blade Profile	NACA4406		
	Solidity	1.245	0.508	0.308
	Stagger Angle	42.40°	60.11°	67.21°
Rear Rotor (RRtype-cal.)	Blade Number	5		
	Blade Profile	NACA4409		
	Solidity	0.91	0.447	0.288
	Stagger Angle	55.92°	63.91°	68.87°

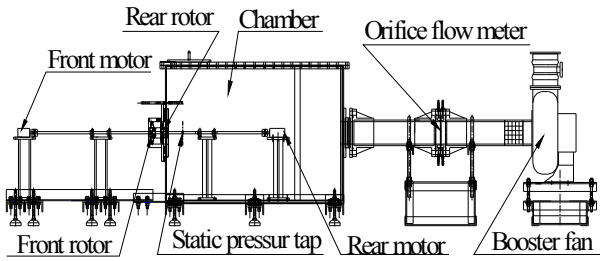

Fig.2 Experimental apparatus

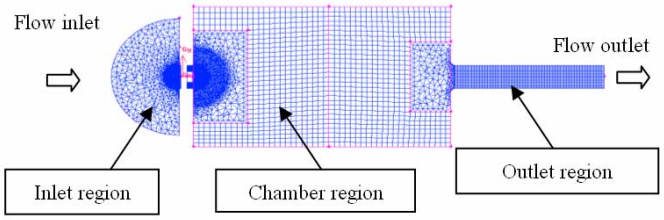

Fig.3 Numerical analysis grids

fan pressure ΔP_{dR}=13.7Pa and ΔP_{dRR}=14.7Pa. Therefore, we need to design the small-sized axial fan considering the fan pressure becomes lower than conventional large size axial fan. The efficiency of RRtype at the designed flow rate Q_d=0.016m^3/s was (η=44.4%) higher than that of Rtype (η=34.8%). Furthermore, the efficiency of RRtype was higher than that of Rtype in all flow rates, where numerical analysis was conducted. On that point, the advantages of the adoption of contra-rotating rotors for small-sized fan were confirmed. It was inevitable to investigate the internal flow condition in order to get better performance of RRtype. Then, the internal flow conditions were investigated by the experiment using a pitot tube and the numerical flow analysis. Figures 5(a) and (b) show the axial and the circumferential velocity distributions at the designed flow rate Q_d in radial direction at the inlet of the front rotor of RRtype respectively. The axial velocity and the circumferential velocity distributions assumed in this design method are shown as a broken line in Fig.5(a) and (b) respectively. The vertical axis is non-dimensional radius divided by the radius at the casing; r/r_c=0.45 and r/r_c=1.0 correspond the hub and the casing. Further, the circumferential velocity V_t/U is a positive in the direction of the front rotor rotation. It was found from Fig.5(a) that the axial velocity increased gradually closing to the inlet of the front rotor and became uniform close to the designed value V_z/U=0.28 at the 5mm upstream of the front rotor inlet. On the other hand, focused on the circumferential velocity in Fig.5(b), the circumferential velocity was almost V_t/U=0 at 5mm upstream of the front rotor inlet and it was observed that flow came in without the circumferential velocity at the inlet of the front rotor and the flow condition at the inlet of the front rotor for RRtype was preferable.

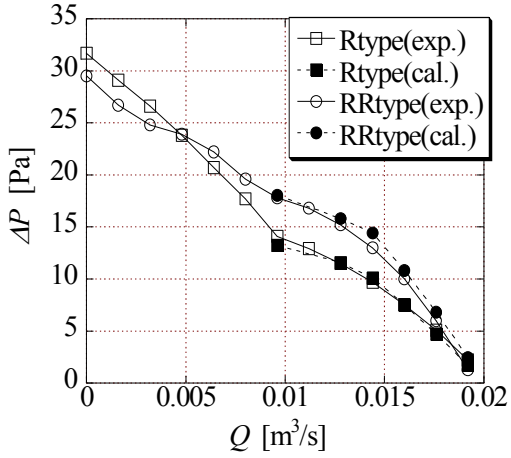

(a) Fan static pressure curves of R and RRtypes

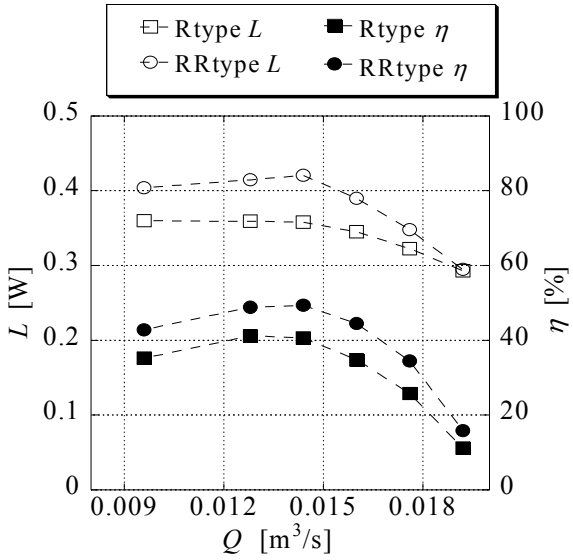

(b) Shaft power and efficiency curves of R and RRtypes (numerical analysis)

Fig.4 Performance curves of of R and RRtypes

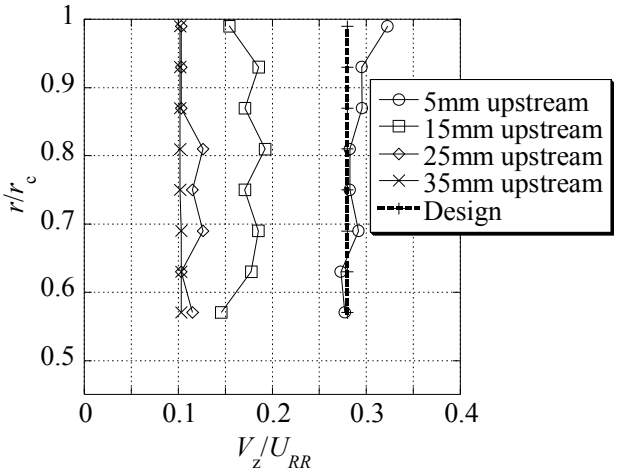

(a) Axial velocity distributions

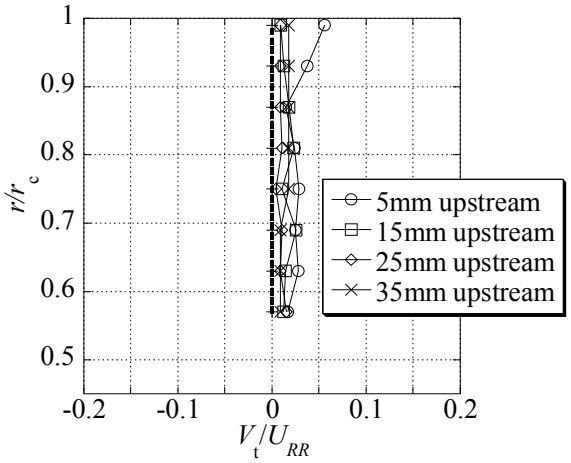

(b) Circumferential velocity distributions

Fig.5 Velocity distributions at the front rotor inlet of RRtype (Q_d=0.016 m^3/s)

It is important for contra-rotating small-sized axial fans to clarify the velocity distributions between the front and the rear rotors because the rear rotor should be designed considering the swirl flow from the front rotor. Figures 6(a) and (b) show the axial and the circumferential velocity distributions of RRtype obtained by the experiment between the front and the rear rotors at the designed flow rate Q_d respectively. Values in a legend are distances of the measurement positions from the front rotor trailing edge at the hub. The axial velocity and the circumferential velocity distributions assumed in this design method are shown as a broken line in Figs.6(a) and (b) respectively . The axial velocity decreased near tip region r/r_c>0.8 between the front and the rear rotors. On the contrary, the axial velocity increased near the hub by the influence of the decrease of the axial velocity near the tip. This would be caused by a inlet shape, a boundary layer near the casing and a leakage flow from the front rotor tip clearance. In the case of small-sized fans, the influence of the boundary layer on a main flow by the low Reynolds number effect and the influence of the leakage flow due to the size effect that the tip clearance become relatively larger than that of large size fans become larger compared to that of the large size fan. Therefore, it was considered that the axial velocity near the tip decreased drastically. The blade-to-blade relative velocity of the front rotor at r/r_c=0.75 and r/r_c=0.98 at the designed flow rate Q_d are shown in Fig.7(a) and (b) respectively. It was observed from Fig.7(b) that a separation occurred on the suction surface near the leading edge of the front rotor even at the designed flow rate Q_d and the leakage flow from the pressure surface to the suction surface near the mid of the blade chord were confirmed. On the other hand, the separation and the leakage flow didn't occur at r/r_c=0.75 and the flow conditions were suitable. The free vortex design was employed on this test fan; rV_t=const. But the circumferential velocity actually increased near the tip as shown in Fig.6(b). This would be caused by the increase of the attack angle near the shroud of the front rotor owing to the decrease of the axial velocity near the shroud. Next, in order to focus on the flow conditions at the inlet of the rear rotor, the attack angle of the rear rotor was evaluated by the numerical results. Figure 8 shows the attack angle distribution at each radial position at the designed flow rate Q_d. The attack angle distribution assumed at the design was depicted as a broken line in Fig.8. The attack angle at each radial position became larger than assumed value at r/r_c=0.8 and the attack angle was larger than assumed value by about 10° near the casing at r/r_c=0.98. It was considered that the increase of the attack angle at the rear rotor was caused by the non-uniform flow condition inclined against hub side at the outlet of the front rotor in Fig.6(a) in addition to the blockage effect by the leakage flow from the rear rotor tip and the boundary layer near the casing. The drastic increase of the attack angle near the shroud caused the fluid loss and a fan performance deteriorated. Therefore, it was important for higher performance of the contra-rotating small-sized axial fan to suppress the leakage flow influence by making the tip clearance

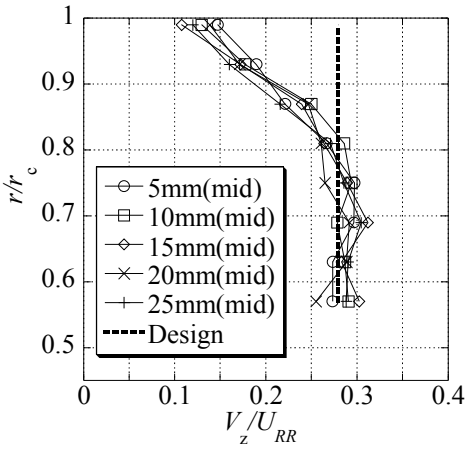

(a) Axial velocity distributions

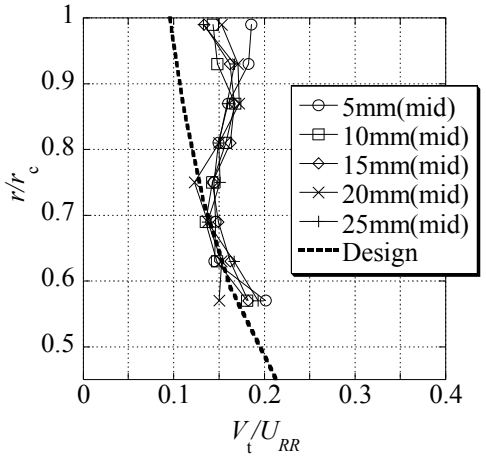

(b) Circumferential velocity distributions

Fig.6 Velocity distributions between the front and the rear rotors of RRtype (Q_d=0.016m^3/s)

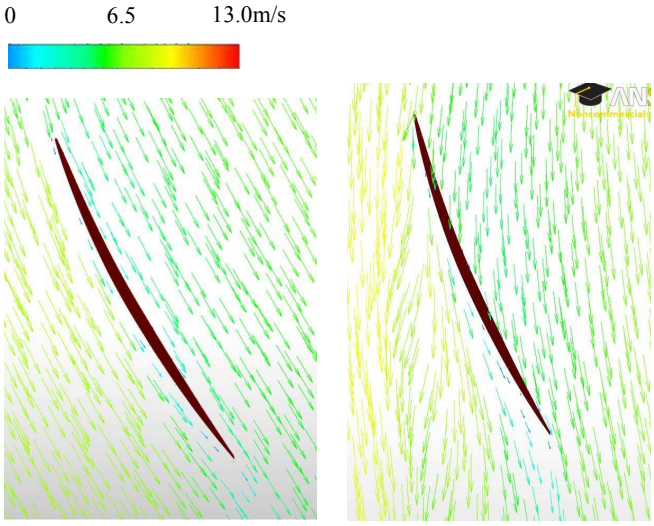

(a) r/r_c=0.75 (b) r/r_c=0.98

Fig.7 Relative velocity vectors around the front rotor of RRtype (Q_d=0.016 m^3/s)

as small as possible and the influence of the boundary layer by increasing the rotational speed. However, there was the restriction to minimize the tip clearance and to increase the rotational speed. Then, it was adequate choice for the performance improvement of RRtype to make the setting angle of the rear rotor near the casing small considering the decrease of the axial velocity near the shroud in addition to the improvement of the inlet shape and the front rotor to make the uniform flow conditions.

The velocity distribution at the outlet of the rear rotor of RRtype at the designed flow rate Q_d was focused. Figures 9(a) and (b) show the axial and the circumferential velocity distributions of RRtype obtained by the experiment at the outlet of the rear rotor at the designed flow rate Q_d respectively. Values in a legend are distances of the measurement positions from the rear rotor trailing edge at the hub. The axial velocity decreased $r/r_c>0.7$ at the outlet of the rear rotor and larger non-uniformity of the axial velocity than that between front and rear rotors in Fig.6(a) was observed. This would be also caused by the flow condition inclined against hub side at the outlet of the front rotor in addition to the blockage effect by the leakage flow from the rear rotor tip and the boundary layer near the casing. On the other hand, the circumferential velocity was almost zero ($V_t/U=0$) at the outlet of the rear rotor for RRtype and it was known the circumferential velocity given by the front rotor was recovered as the static pressure by the rear rotor in the case of RRtype. Further, the mass flow rate averaged total (P_t), static (P_s) and dynamic pressure (P_d) distributions in axial direction of R and RRtypes are shown in Fig.10. The horizontal axis of Fig.10 shows the non-dimensional axial distance evaluated by the axial distance from the leading edge of the front rotor at the hub divided by the chord length at the rear rotor hub. It was seen from Fig.10 that the gentle slope of the pressure increase for RRtype compared to that of Rtype. Furthermore, the total pressure decrease downstream of the rear rotor of RRtype was lower than that of Rtype. The effect of the pressure recovery by the rear rotor of the contra-rotating small-sized axial fan shown in Fig.9(b) was confirmed from these results.

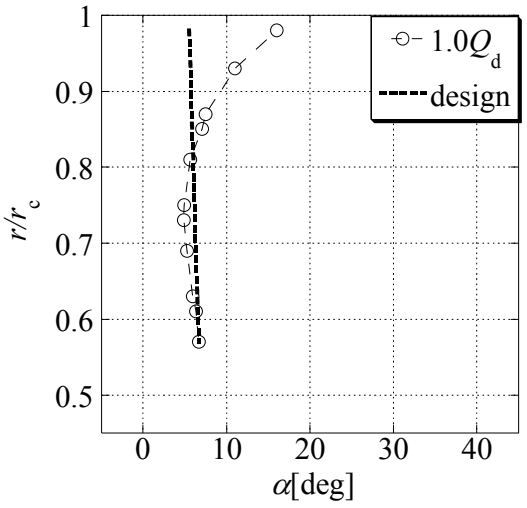

Fig.8 Attack angle distribution of the rear rotor for RRtype (Q_d=0.016 m^3/s)

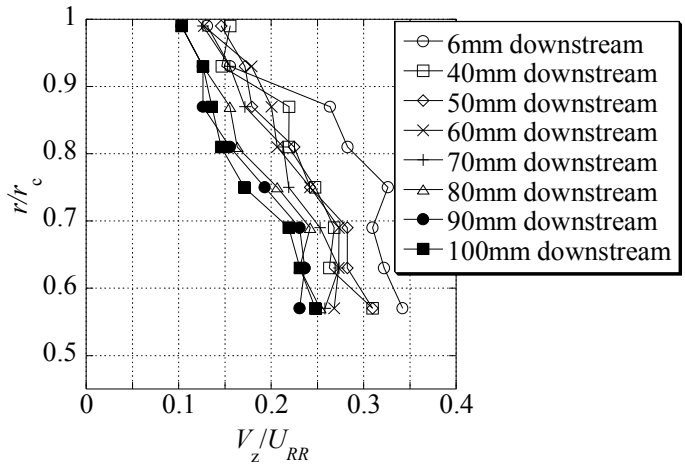

(a) Axial velocity distributions

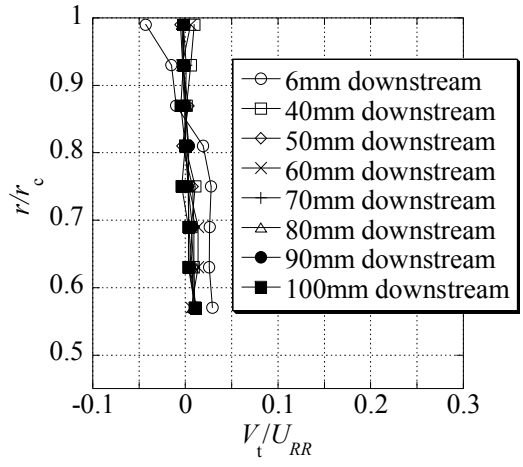

(b) Circumferential velocity distributions

Fig.9 Velocity distributions at the rear rotor outlet of RRtype (Q_d=0.016 m^3/s)

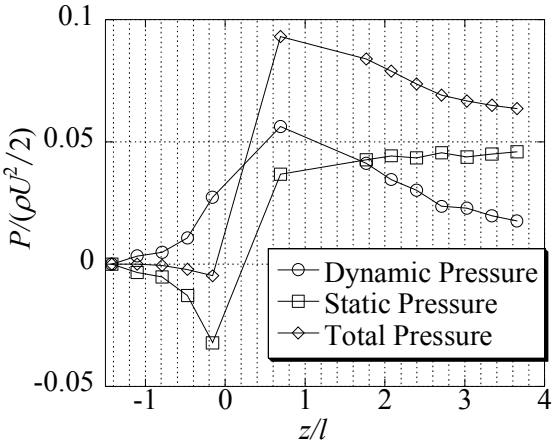

(a) Rtype

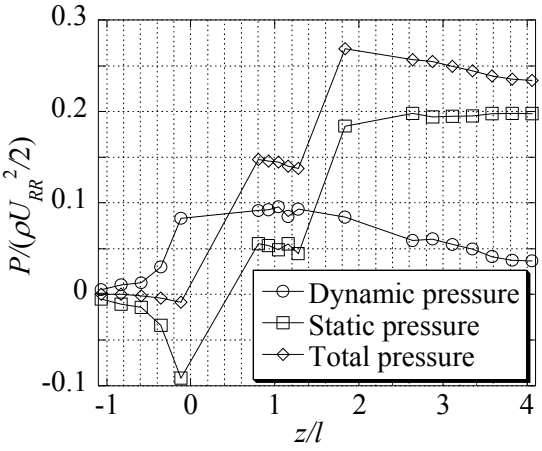

(b) RRtype

Fig.10 Axial distributions of each pressure increase (Q_d=0.016 m^3/s)

CONCLUDING REMARKS

The performance and the internal flow conditions at the designed flow rate of the contra-rotating small-sized axial fan were investigated by the experiment and the numerical analysis. As a result, following concluding remarks were obtained.

1) The fan static pressure curve of this test contra-rotating small-sized axial fan with 100mm diameter showed the stable gentle slope.
2) The axial velocity between the front and the rear rotors near the casing decreased by the inlet shape, the boundary layer near the casing and the leakage flow from the blade tip. As a result, the attack angle of the rear rotor near the casing increased and fluid loss was caused.
3) In order to improve the performance of this test fan(RRtype), it is important to decrease the setting angle of the rear rotor near the casing considering the decrease of the axial velocity near the casing at the outlet of the front rotor in addition to the improvement of the inlet shape and the front rotor to make the uniform flow conditions.

ACKNOWLEDGEMENT

The authors wish to show our special thanks to the supports by the project research aid from The University of Tokushima, Japan Science and Technology Agency and Komiya research aid.

REFERENCES

1. Miyahara, M and Fukano, T., Fan Cooling Technology for Small Electronic Device, *Turbomachinery*(in Japanese), Vol. 34, No3, (2006), pp.129-134.
2. Furukawa, A., Shigemitsu, T and Watanabe, S., Performance Test and Flow Measurement of Contra-Rotating Axial Flow Pump, *J. Thermal Science*, Vol.16, No.1, (2007), pp.7-13.
3. Furukawa, A., Cao, Y., Okuma, K and Watanabe, S., Experimental Study of Pump Characteristics of Contra-Rotating Axial Flow Pump, *Proc. 2nd Int. Symp. on Fluid Machinery and Fluid Eng.,* Beijing, 67-657, (2000), pp.245-252.
4. Kodama, Y., Hayashi, H., Fukano, T and Tanaka, K., Experimental Study on the Characteristics of Fluid Dynamics and noise of a Counter-Rotating Fan(1st Report, Effects of the Supporter Shape of the Electric Motor and the Distance between Two Rotors on the Characteristics), *Trans. JSME* (in Japanese), Vol. 60, No. 576, (1994), pp.2764-2771.
5. Shigemitsu, T., Furukawa, A., Okuma, K and Watanabe, S., Experimental Study on Rear Rotor Design in Contra-Rotating Axial Flow Pump, *Proc. 5th JSME/KSME Fluids Eng. Conf.*, Nagoya, (2002), pp.1453-1548.
6. Sanders, A, J., Papalia, J and Fleeter, S., Multi-Blade Row Interactions in a Transonic Axial Compressor: Part I- Stator Particle Image Velocimetry (PIV) Investigation, *ASME J. Turbomachinery*, Vol.124, (2002), pp.10-18.
7. Shigemitsu, T., Fukutomi, J., Yano, T and Okabe, Yuki., The Performance and The Similarity Law of Small-Sized Axial Fan and The Possibility of Adoption of Contra-Rotating Rotors, *Proc. 9th Int. Symp. on Experimental and Computational Aerothermodynamics of Internal Flows*., Gyeongju, (2009), CD-ROM.
8. Ito, T., Minorikawa, G,. Nagamatsu, A and Suzuki, S., Experimental Research for Performance and Noise of Small Axial Flow Fan(influence of Parameter of Blade), *Trans. JSME* (in Japanese), Vol. 72, No. 715, (2006), pp.670-677.